Chromosome elasticity and mitotic polar ejection force measured in living *Drosophila* embryos by four-dimensional microscopy-based motion analysis

Wallace F. Marshall*‡, John F. Marko†, David A. Agard* and John W. Sedat*

Background: Mitosis involves the interaction of many different components, including chromatin, microtubules, and motor proteins. Dissecting the mechanics of mitosis requires methods of studying not just each component in isolation, but also the entire ensemble of components in its full complexity in genetically tractable model organisms.

Results: We have developed a mathematical framework for analyzing motion in four-dimensional microscopy data sets that allows us to measure elasticity, viscosity, and forces by tracking the conformational movements of mitotic chromosomes. We have used this approach to measure, for the first time, the basic biophysical parameters of mitosis in wild-type *Drosophila melanogaster* embryos. We found that *Drosophila* embryo chromosomes are significantly less rigid than the much larger chromosomes of vertebrates. Anaphase kinetochore force and nucleoplasmic viscosity were comparable with previous estimates in other species. Motion analysis also allowed us to measure the magnitude of the polar ejection force exerted on chromosome arms during metaphase by individual microtubules. We find the magnitude of this force to be approximately 1 pN, a number consistent with force generation either by collision of growing microtubules with chromosomes or by single kinesin motors.

Conclusions: Motion analysis allows noninvasive mechanical measurements to be made in complex systems. This approach should allow the functional effects of *Drosophila* mitotic mutants on chromosome condensation, kinetochore forces, and the polar ejection force to be determined.

Addresses: *Department of Biochemistry and Biophysics, University of California San Francisco, San Francisco, California 94143, USA. †Department of Physics, University of Illinois at Chicago, Chicago, Illinois 60607, USA.

Current Address: ‡Molecular, Cellular, and Developmental Biology Department, Yale University, New Haven, Connecticut 06520, USA.

Correspondence: Wallace Marshall
E-mail: wallace.marshall@yale.edu

Received: **12 January 2001**
Revised: **5 March 2001**
Accepted: **5 March 2001**

Published: **17 April 2001**

Current Biology 2001, 11:569–578

0960-9822/01/$ – see front matter
© 2001 Elsevier Science Ltd. All rights reserved.

Background

A major challenge of modern cell biology is to study complex systems in an intact state. In the postgenomic era, the dissection of cellular processes at the molecular level will soon become so complete that the most important remaining questions in cell biology will no longer directly concern molecules themselves, but rather the emergent properties that result from interactions within large networks of molecules. Gene array expression-profiling technologies have begun to address such interactions at the level of logic and information flow, for instance in transcriptional regulatory networks, by allowing simultaneous analysis of time-varying expression levels for large numbers of genes in vivo. But many cellular processes, such as motility and cell division, are less informational and more mechanical in nature, so that there remains a pressing need for comparable tools to simultaneously analyze mechanical interactions of large numbers of cellular components in intact cells.

Four-dimensional (4D) microscopy, the acquisition of time-lapse three-dimensional image sequences [1–4], provides an excellent opportunity to collect massive datasets revealing movements in living cells. These data are potentially a rich source of information about mechanics because movements seen in such images reflect the underlying mechanics. But this poses a formidable bioinformatics challenge — how to extract meaningful quantitative information about mechanics from 4D image sequences. The current availability of several commercial 4D microscopy systems, and the low cost of computer power, suggest that the time is now ripe to answer this challenge.

Our initial efforts to measure cellular mechanics from 4D image data have focused on mitosis. Mitosis is an essentially mechanical process, and mechanical measurements using micromanipulation have been crucial in advancing our understanding of its mechanism. Unfortunately, the cells most amenable to direct micromanipulation, such as grasshopper spermatocytes, are not genetically tractable, while the nuclei of major genetic model

organisms, such as *Drosophila*, are so small and compact as to make micromanipulation experiments virtually impossible. Moreover, micromanipulation is invasive and raises concerns about perturbations to the system, and it is inherently limited to measuring forces at one or two positions and thus cannot be used to make simultaneous measurements throughout an entire cell.

We have developed a set of computational tools to derive mechanical measurements from noninvasive observation of three-dimensional movements of mitotic chromosomes in live cells. Using our 4D motion analysis approach, we have measured the fundamental mechanical properties characterizing mitosis in *Drosophila* embryos. These properties include chromosome flexibility, kinetochore force, nucleoplasmic viscosity, and the polar ejection force. The values we obtained for kinetochore force and nucleoplasmic viscosity are comparable to measurements previously reported in careful studies on newt lung epithelia [5–7] and grasshopper spermatocytes [8, 9], while elasticity measurements indicated that *Drosophila* embryo chromosomes were much less rigid than grasshopper or newt chromosomes. In addition to these measurements, which have previously been made on other organisms, our approach also allowed us to measure the magnitude of the individual force-generating events underlying the polar ejection force. The magnitude of polar ejection force obtained by this analysis is consistent with that generated by the polymerization of single microtubules or by single kinesin motors.

This approach opens the door to combining 4D analysis with the power of *Drosophila* genetics to study how individual gene products contribute to the biomechanics of mitosis. Our technique is of course not limited to chromosomes, and thus the present report defines a new way to use microscopy to study in vivo subcellular biomechanics.

Figure 1

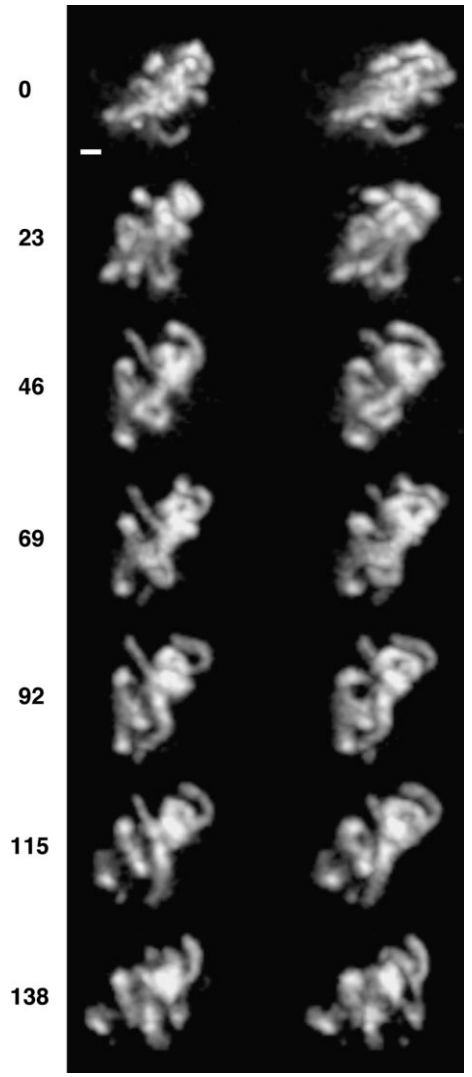

Time-lapse three-dimensional images of chromosomes in living *Drosophila* embryos are viewed as stereo pairs. The scale bar represents 2 μm.

Results

Computational analysis of four-dimensional chromosome motion

Our basic approach is to infer the dynamics of chromosomes, i.e., the forces acting on them, from their kinematics; that is, their observed movements. The essential first step is to collect quantitative motion data. We visualize chromosomes in vivo by injecting *Drosophila* embryos with fluorescently labeled histone protein [2] and collect images using four-dimensional widefield-deconvolution fluorescence microscopy (see Materials and methods). This results in a time-lapse series of three-dimensional images in which the chromosomes are clearly resolved (Figure 1).

To analyze motion in these images, we have developed an algorithm (Figure 2) capable of tracking the movements of a set of nonrigid chromosome-like objects (see Materials and methods). Computational motion estimation has previously been used with great success to track chromosome movements [10], but the block-matching optical flow algorithm employed was limited to tracking chromosome segments such as kinetochores, which appeared visually distinct from the rest of the chromosome. Most segments of a mitotic chromosome arm look identical and cannot be tracked by such a pattern-based motion analysis algorithm. In our approach, we interactively trace the chromosome in three-dimensional images to find curves that each represent a single chromosome (Figure 3). The motion estimation problem then reduces to a matching problem in which we attempt to find the optimal mapping between the set of curves at time t and the set of curves at time t + 1 (see Materials and methods). From this mapping

Figure 2

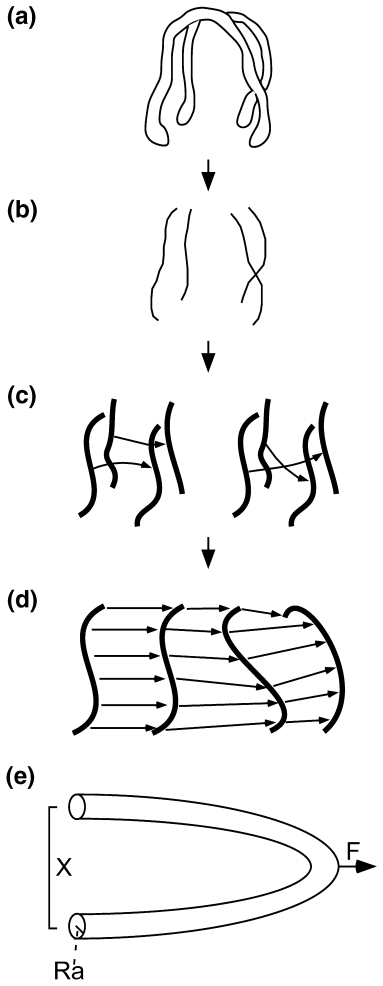

Schematic outline of the motion analysis procedure. **(a)** First, three-dimensional chromosome images are obtained for each time point. **(b)** Chromosome backbone curves are traced interactively to represent the shape and position of each chromosome. **(c)** Starting with the set of backbone traces for every time point, every possible mapping of chromosomes at time t onto chromosomes at time t + 1 is evaluated to find the optimal mapping. In the example shown in this figure, there are just two chromosomes, and the diagram shows the two ways to trace arms at time t onto arms at time t + 1, as signified by the arrows. **(d)** Given the optimal mapping for each time interval, the motion of each chromosome arm can be traced through the entire time series. This allows one to measure elasticity by measuring curvature fluctuations at individual points on a chromosome over time. **(e)** Calculation of anaphase force F from the shape of anaphase chromosomes in terms of the chromosome radius Ra and the through-space distance between telomeres X. See Equation 3 in the text.

we can determine the three-dimensional movements of every point on every chromosome. The resulting set of motion vectors is a rich source of mechanical data, implicitly containing enough information to compute chromosome elasticity, kinetochore force, and effective nuclear viscosity.

Chromosome elasticity

Chromosome elasticity is a quantitative reflection of the interactions that hold the chromosome together, and it can thus provide physical insights into mitotic chromosome architecture. Using our motion analysis results, we can measure chromosome elasticity based on the thermally driven fluctuations in chromosome curvature. A similar approach has previously been used to measure elasticity of microtubules [11] and in vitro assembled *Xenopus* chromatin [12]. One complicating factor in making such measurements on mitotic chromosomes in vivo is that it is expected that the polar ejection force, by randomly pushing the chromosome arms around, causes curvature fluctuations above and beyond those caused by collisions with thermally excited solvent particles. To circumvent this complication, we injected embryos with colchicine to depolymerize all microtubules. We saw that the chromosome bending motions were substantially reduced by this treatment, and we assumed that any remaining movements were thermal fluctuations, i.e., were due to collisions with thermally excited solvent molecules. These experiments were all done at metaphase.

The bending angle θ at each point is defined by the angle between successive tangent vectors spaced 1 μm apart (see Materials and methods), and we computed the variance of this angle over time. The thermally-driven variance in bending angle (in radians) of an elastic rod [13] is given by

$$<\Delta\theta^2(s)> = 2skT/B \qquad (1)$$

where s is the arc length between tangent vectors (1 μm), k is Boltzmann's constant (1.4×10^{-23} J/K), T is the absolute temperature, and B is the bending modulus. Our measured value for the variance in bending angle from chromosomes in embryos injected with colchicine is 0.013 ± 0.004, from which it follows by Equation 1 that the bending modulus is $B = 6.2 \times 10^{-25} \pm 2 \times 10^{-25}$ J·m (equivalently, N·m^2). The "thermal persistence length" of a *Drosophila* chromosome (the length over which approximately one radian bend occurs), is just $B/(kT) = 1.5 \times 10^{-4}$ m.

For comparison, the bending modulus for microtubules is about 10^{-23} J·m, while that for actin is approximately 10^{-25} J·m. Thus, *Drosophila* chromosomes are more flexible than the individual microtubules that push on them. We also found that the variance in the bending angle for chromosomes in metaphase cells untreated with colchicine was 0.062 ± 0.003, implying that chromosomes undergo much more extensive bending in the presence of microtubules (see below).

From the bending modulus we can obtain the Young's modulus, Y, which is a size- and shape-independent measure of the intrinsic elasticity of a material, in this case

Figure 3

Representation of chromosome conformation. We obtained this representation by tracing the backbone of chromosome arms. Left panel, stereo pair images of chromosomes at successive time points. Right panel, corresponding representation of chromosome complements as a set of curves, obtained by interactive tracing.

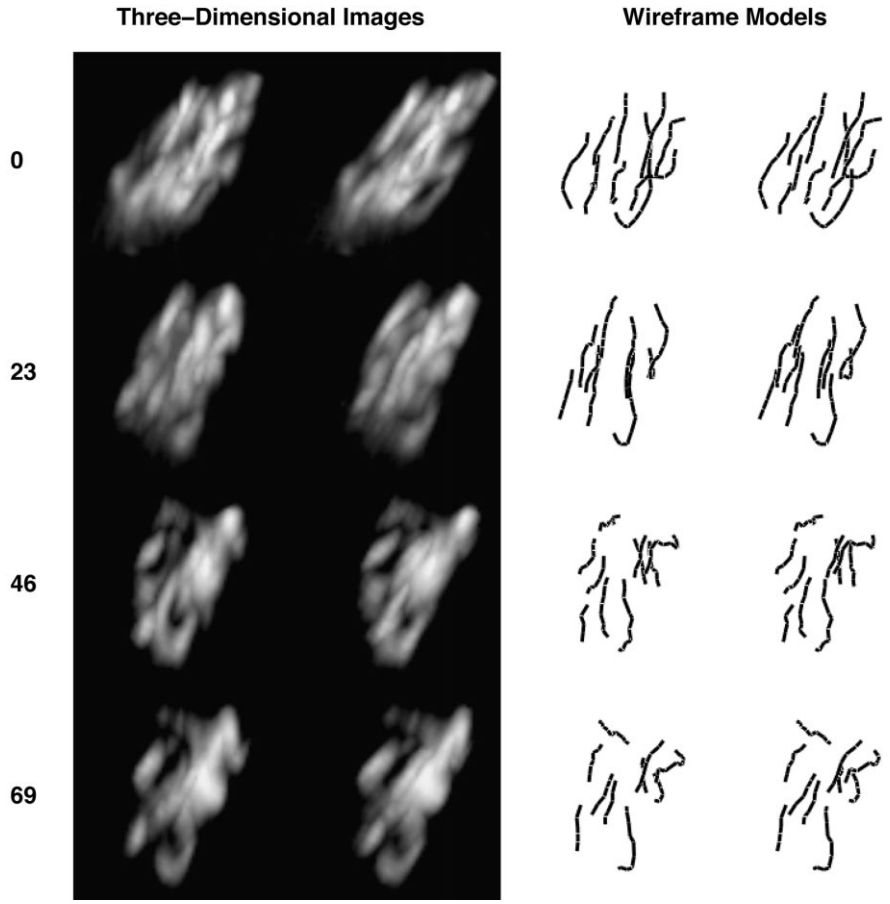

condensed chromatin. For a cylinder of radius R, the Young's modulus Y is related to the bending modulus B by the relation

$$Y = 4B/\pi R^4 \quad (2)$$

For metaphase chromosomes in embryos injected with colchicine, R is measured to be 0.38 ± 0.04 μm, so Equation 2 gives a Young's modulus of 38 ± 20 Pa. We note that this calculation assumes that the chromosomes are isotropic and cylindrical. Although metaphase chromosomes are in fact a pair of parallel sister chromatids, under our imaging conditions we cannot resolve the pair, and the chromosomes appear cylindrical.

By comparison, micromanipulation experiments [9] indicated a Young's modulus of 430 Pa for grasshopper chromosomes. Experiments using micropipette aspiration [6] gave an upper bound of 1000 Pa for prometaphase newt chromosomes; more recent static mechanical measurements on the same system gave a modulus of 250 Pa [7]. The lower Young's modulus for *Drosophila* embryo chromosomes may imply that they are less compact than in other species, possibly a result of the extremely short duration of mitosis.

Anaphase kinetochore force

The forces exerted by the spindle on the kinetochore provide insights into the molecular mechanism of force generation. Based on the observed shape of anaphase chromosomes, we can use Young's modulus to compute the force pulling on the kinetochore in anaphase. This method has recently been described by Houchmandzadeh et al. [6], who show that to a first approximation

$$F = 6\pi Y R_a^4/X^2 \quad (3)$$

where F is the anaphase kinetochore force, R_a is the radius of the anaphase chromosome, and X is the through-space distance between the chromosome ends (Figure 2e). In three-dimensional images of anaphase chromosomes, we have measured the average distance between anaphase chromosome ends to be X = 1.15 ± 0.26 μm, and we measured the average radius of an anaphase chromosome

to be $R_a = 0.19 \pm 0.04$ μm. In order to avoid any effects due to resistance from sister chromosome connections, we only made measurements on nuclei in which the pairs of chromatids could be seen to have separated completely. Given our measured value for Y of 38 Pa, from Equation 3 we calculated the average force pulling on the kinetochore in anaphase to be $F = 0.7 \pm 0.4$ pN. We note that this analysis assumes that the bending modulus of the chromosome is constant along its length. This assumption is likely to be not strictly correct since the chromosome may be significantly more flexible in the region of the centromere. The anaphase force estimate reported here should therefore be treated as an upper bound; if the centromere region of the chromosome is more flexible than the arms, then a smaller force would be able to lead to the same reduction in the through-space distance between the telomeres. This same anaphase chromosome shape analysis was used in newt lung epithelial cells [6] and, combined with the value for the Young's modulus of mitotic newt chromosomes of 250 Pa [7], yields an upper bound on the anaphase force in newt cells of 250 pN. The much larger force observed for newt cells may correlate with the much larger overall cell, spindle and chromosome sizes, relative to those of *Drosophila*, although the value for newt chromosomes, like the value reported here for *Drosophila*, must be treated as an upper bound on the anaphase force given our lack of knowledge of the flexibility of the centromere region.

A previous estimate of spindle force of 0.1 pN was obtained for grasshopper cells by Nicklas [8], who multiplied the anaphase velocity by an estimated friction coefficient that he obtained by assuming an effective viscosity of 100 cP (1 cP = 10^{-3} Pa·sec), a value 100 times greater than the viscosity of water. In an elegant study of mitosis in newt cells, Alexander and Rieder [5] used the same approach to obtain a spindle force of 10 pN during early prometaphase, but in this case they inferred an average viscosity of 282 cP by measuring the Brownian motion of 0.4 μm particles in the cytoplasm. To make a strict comparison, we note that the 10 pN force measured by Alexander and Rieder were based on rapid prometaphase chromosome movements, which occur with a velocity roughly 10 times greater than in anaphase. This suggests that the anaphase kinetochore force in newt cells is probably on the order of 1 pN rather than 10 pN. Thus, our value of 0.7 pN is quite comparable to these previously reported values. Interestingly, in all cases the anaphase kinetochore force estimates were several orders of magnitude smaller than the maximum force that a kinetochore can exert, which Nicklas measured to be 700 pN [9]. We note that our measurement technique has the advantage that it does not rely on an independent estimate for the viscosity, which can in principle be strongly size dependent [14]. Using this alternative approach, we still obtain an upper bound on the force in anaphase that is several orders of magnitude less than the maximum stall force of the kinetochore. These findings thus support the conclusion that kinetochores are able to generate far larger forces than they typically do.

Nucleoplasmic viscosity

The viscosity of the nucleoplasm plays an important role in determining the displacements produced by forces acting on chromosomes. Viscosity also provides an indication of the physical environment within the nucleus. We note that the effective viscosity in the region of the mitotic spindle could well be different from that of the surrounding cytoplasm due to hindrance both by the components of the spindle itself and by additional protein structures, such as the insoluble network of CP60 and CP190 that remains in the nucleus during mitosis in *Drosophila* embryos [15]. The viscosity experienced by chromosomes in situ relative to that experienced in solution thus provides an indicator of large-scale structure in the spindle.

During anaphase, the chromosome movement caused by the kinetochore force F is resisted by viscous drag due to the movement of the chromosomes through the nucleoplasm. For movement at constant velocity, the kinetochore force is exactly balanced by the drag force. This leads to the relation

$$F = \xi v \tag{4}$$

where ξ is the frictional drag coefficient and v is the velocity. Based on measured displacements between successive images during anaphase, we estimate the average velocity of anaphase chromosomes in *Drosophila* to be 1.4×10^{-7} ms^{-1}. Therefore, given F = 0.7 pN, by Equation 4 the frictional coefficient is $\xi = 5 \times 10^{-6}$ Kg s^{-1}.

For an ellipsoid that is dragged end-on through a viscous liquid medium, the frictional coefficient can be related to the viscosity by the relation

$$\xi = 4\pi\eta a/[\ln (2a/b) - 0.5] \tag{5}$$

where η is the viscosity, a is half the length of the ellipsoid, and b is the radius [16]. *Drosophila* has a haploid complement of three major chromosomes, two of which (chromosome 2 and chromosome 3) are metacentric and one of which (X) is telocentric. The anaphase force estimates were based on the shape of metacentric chromosomes only. All anaphase chromosome arms in *Drosophila* are 6 μm long, regardless of whether they are on telocentric or metacentric chromosomes, so a = 3 μm, and the radius b is just the radius R_a measured for anaphase chromosomes, 0.19 μm. For a metacentric chromosome, a given kinetochore would be dragging two such arms through the medium, so the effective frictional coefficient will be twice that given by Equation 5. From these considerations we find that metacentric anaphase chromosomes behave as though they are moving in a liquid medium with an effective viscosity $\eta = 0.2$ Pa·sec (or 200 cP). For compari-

son, we note that the viscosity of water is 1×10^{-3} Pa·sec. Our viscosity measurement is virtually identical to the average viscosity of 282 cP previously estimated based on Brownian movements of small particles in the vicinity of the spindle [5]. This finding thus indicates that the prometaphase force estimates calculated by Alexander and Rieder based on this viscosity are likely to be correct. However, as discussed above, our estimated anaphase kinetochore force should be treated as an upper bound, and therefore our viscosity estimate must also be treated as an upper bound; the actual nucleoplasmic viscosity could be lower.

Magnitude of the polar ejection force

The polar ejection force remains one of the least understood aspects of mitosis. There are presently two models to account for this force. One possibility is that chromosome-associated kinesin motor proteins may generate the ejection force [17–20]. Alternatively, it has been proposed that the ejection force could arise due to collisions with growing microtubules [21, 22]. We set out to test the microtubule polymerization mechanism by asking whether the force generated by a single polymerizing microtubule could be sufficient to account for the polar ejection force. If the ejection force generated by a microtubule exceeded the maximum force of microtubule polymerization, this would argue strongly in favor of a motor-based mechanism.

This approach requires a way to measure the components of the ejection force generated by individual microtubule-chromosome interactions. It is therefore not sufficient to just measure the overall resulting movement of the whole chromosome. The fact that chromosome curvature fluctuations are greater in the presence of microtubules (see above) implies that the individual force generation events underlying the polar ejection force exert random forces whose magnitude is significant compared to the forces exerted by collisions with thermally excited solvent particles (Brownian motion). This suggests a way to estimate the magnitude of the contributions to the polar ejection force from each microtubule, namely treating them as Langevin random forces, analogous to those exerted by solvent particles during Brownian motion. We can use this Langevin approach to relate fluctuations in curvature to the magnitude of the applied random force.

To compare curvature fluctuations in the presence or absence of microtubules, we measured the persistence length (see Materials and methods), which is a measure of the spatial scale over which bending motions are correlated. By comparing the persistence length in normal embryos to those in which the microtubules were depolymerized by the injection of colchicine, we could estimate the magnitude of individual polar ejection force-generating events. For an elastic rod experiencing a set of random forces, the apparent persistence length $\rho_{apparent}$ is reduced from its purely thermal value $\rho_{thermal}$ such that

$$\rho_{thermal} / \rho_{apparent} = 1 + f^2\tau/kT\lambda\eta \quad (6)$$

where f is the magnitude of the random force, λ and τ are the spatial correlation length and temporal correlation times of the force, and η is the viscosity (see Materials and methods for derivation).

The spatial correlation distance λ can be approximated as the average distance between adjacent microtubules contacting a given chromosome. We take this distance to be in the order of 1 μm based on electron micrographs of *Drosophila* embryo centrosomes [23] and fluorescence images of *Drosophila* embryos during mitosis [24]. Considering a simple model for force generation by growth of microtubules, we take τ to be the time between additions of subunits on individual microtubules. Assuming individual microtubules in vivo grow at the previously measured rate of 14.3 μm/min [25], and given that for a thirteen-protofilament microtubule the addition of a single αβ tubulin dimer would cause the microtubule to elongate by 0.6 nm, we obtained an average time between dimer additions of $\tau = 2.5$ ms.

Based on our calculations, we found that in the presence of microtubules, the persistence length is reduced from 154 μm to 32 μm (see Materials and methods, Equation 10), a factor of 4.8. Inserting these values into Equation 6, we estimate that the magnitude of individual polar ejection forces is approximately 1.1 pN. This force is in the range generated by single kinesin motors [26–28], but it is also comparable to the force that can be generated by polymerization of a single microtubule (2–4 pN [29–30]). We therefore conclude that the magnitude of the polar ejection force is equally compatible with either a simple microtubule polymerization-driven mechanism or a kinesin motor-based mechanism.

This estimate of the ejection force should be treated as an upper bound; that is, the actual ejection force could be even lower. One reason is that, in addition to the ejection force, kinetochore movements also contribute to the apparent bending motions of the chromosomes, so that the component of the bending fluctuations that is due purely to the polar ejection force may be somewhat less than the total bending fluctuations observed. Another reason our estimate should be treated as an upper bound is that we have used a τ corresponding to single tubulin dimer addition. If τ were larger, e.g., if multiple dimers were added during one event, a smaller value for the ejection force would result. Finally, as discussed above, the viscosity estimate employed here is itself an upper bound on the actual viscosity, and if the viscosity were lower, a correspondingly lower ejection force magnitude would suffice to generate the fluctuations observed. We stress that even our maximum upper bound for the ejec-

Table 1

Chromosome mechanics

Organism	Young's Modulus (Pa)	$F_{kinetochore}$ (pN)	Viscosity (cP)
Grasshopper	430	0.1	100
Newt	250	1.0	282
Drosophila	38	0.7	200

Chromosome mechanics during the rapid mitosis of *Drosophila* compared with the slower divisions of newt mitosis [5, 6, 7] and grasshopper meiosis II [8, 9].

tion force magnitude is still consistent with known microtubule polymerization forces, so that even if the ejection force were significantly lower than our estimate it would not change our fundamental conclusion that the magnitude of this force is compatible with either motor- or polymerization-driven force generation.

Discussion

Chromosome mechanical measurements in a genetic model organism

Our four-dimensional motion analysis approach has allowed us to make the first mechanical measurements on mitotic chromosomes in *Drosophila* embryos. Mitosis in *Drosophila* embryos has always been considered unusual because of its speed. The entire process from nuclear envelope breakdown to nuclear reassembly takes less than 30 min. One might expect that the short time allotted for chromosome condensation might result in a less rigid chromosome. Likewise, greater forces might be exerted during anaphase to reduce the time spent pulling chromosomes apart. Table 1 compares the chromosome elasticity and anaphase kinetochore force that we have measured in *Drosophila* with measurements of the same parameters in newts and grasshoppers [5–9]. As predicted, *Drosophila* chromosomes appear to be significantly more flexible than the larger chromosomes of newts or grasshoppers, as reflected in the smaller Young's modulus. This presumably indicates that *Drosophila* embryo chromosomes may be less tightly compacted. On the other hand, the kinetochore force lies roughly within the range of values observed in newts and grasshoppers.

The power of *Drosophila* genetics allows the identification of mitotic mutants and reveals gene products that play a role in mitosis [31]. Given that mitosis is a fundamentally mechanical process, many of these gene products are likely to play a predominantly mechanical role, either by exerting forces directly on the kinetochores or indirectly on the arms or by acting as structural components of the spindle or chromosomes. Our approach for measuring these mechanical properties in *Drosophila* is relatively noninvasive and easy to carry out. Thus, it should be quite feasible to apply this analysis to the entire collection of *Drosophila* mitotic mutants and to ask which genes play roles in kinetochore force generation (as derived from the anaphase configuration), polar ejection force generation (as calculated from the difference in curvature fluctuations in the presence and absence of microtubules), spindle assembly (as reflected in the apparent viscosity), or chromosome condensation (as measured by Young's modulus).

Beyond imaging: A computational approach to cellular mechanics

Microscopy is usually viewed as a method for determining the position or shape of cellular structures. We emphasize that data obtained from modern multidimensional time-lapse microscopy on living cells also contains information about forces and elastic properties. In particular, the conformational dynamics of cellular structures provides a direct indication of their mechanical properties. The present work illustrates one example of how intracellular forces can be calculated from the movement of subcellular structures. This type of kinematic analysis has proven invaluable in astronomy, for example in determining the principles governing the motion of planets, a case obviously not amenable to direct experimental manipulation. When applied to cell biology, this approach gives us potentially large advantages in circumventing the difficulties and potential artifacts of micromanipulation. We and others [5, 8, 10] have shown this to be the case for chromosome mechanics, and a recent study has shown the power of motion analysis in studying the transport of vesicles [32]. Within the next decade, we expect that the determination of mechanics from motion analysis will become a routine cell biological tool.

Materials and methods

In vivo chromosome imaging

Drosophila embryos (Oregon R) were injected with Cy5-labeled histone protein as previously described [2, 24]. Colchicine treatment was performed by colchicine coinjection at a concentration of 200 mg/ml along with the labeled histones. This caused embryos to arrest in metaphase with condensed chromosomes. After waiting 30 min to allow histone incorporation, we scanned embryos to find ones just entering the 12th mitosis (as judged by the number of nuclei in one field of view). Three-dimensional data sets were acquired by widefield fluorescence microscopy at a rate of one 3D data set every 23.4 s. At each time interval, 18 optical sections spaced 0.25 μm apart were collected with a cooled CCD. Sections were 256 × 256 pixels in size, each pixel representing 0.1 μm on a side. Labeling and imaging did not perturb the embryo; after imaging, embryos were maintained in humid chambers and found to develop and hatch normally and on time at the same rate as control embryos injected with buffer and not imaged. During imaging, successive mitoses remained synchronized, and abnormalities indicative of DNA damage, such as anaphase bridges, were not observed. Following data collection, out-of-focus light was removed by constrained iterative deconvolution [33]. 4D image visualization and manipulation was done with the IVE software platform [34]. We interactively traced chromosome arms by using interactive modeling software [34] to provide backbone traces. Backbone tracing is done manually by stepping through optical sections and using a cursor to designate the apparent center of the chromosome in each section. Successive center points are stored in a list and used to define the backbone path. We note that while in principle the metaphase chromosome is actually a pair of parallel sister chromatids, under our imaging conditions we cannot resolve the two sisters, and the chromosome generally looks cylindrical in cross section.

Algorithm for three-dimensional nonrigid motion analysis

We have previously described an algorithm for tracking the motion of a set of nonrigid, elongated objects such as chromosomes by using simulated annealing [35]. Each object was represented as a backbone trace, which reduced the motion estimation problem to a problem of mapping one set of curves onto another. The correct mapping was defined as that which minimized the total mean-squared displacement between all mapped curves.

In the current implementation of this algorithm (Figure 2), backbones are interactively traced for each chromosome arm, and then the trace is resampled at uniform intervals of 0.1 μm along the curve. For chromosome arm m at time t, we define the position of the chromosome segment at interval i along the arm by the position vector r(m, t, i). The number of intervals sampled for a given arm m at time t is N(m, t). Next, we individually consider every possible pair (m, n) of chromosomes arms at time t and t + 1, respectively, and compute the mean-squared distance between the arms as

$$d(m, t; n, t + 1) = (1/N_{min}) \sum_{j=1}^{N_{min}} || r(m, t, j) - r(n, t + 1, j) ||^2 \quad (7)$$

where $N_{min} = \min[N(m, t), N(n, t + 1)]$. We now consider the entire set A(t) of chromosome arms at time t. The solution to the motion estimation problem will be a mapping f of arms at time t onto arms at time t + 1, $f:A(t) \rightarrow A(t + 1)$ so that given a mapping, we say that arm m at time t maps onto arm f(m) at time t + 1. We define the optimal mapping f_{opt} as the one that minimizes the total mean-squared distance

$$d_{tot} = \sum_{m=1}^{c} d(m, t, f(m), t + 1) \quad (8)$$

To find f_{opt} at each time interval, we iteratively compute the value of d_{tot} for every possible mapping f.

Once we obtain the optimal mapping, it becomes possible to track the value of any function of position along the arm, such as curvature, and measure its fluctuations over time. For computing fluctuations in curvature we determine curvature by a simple sliding-leg technique. For each point i on a chromosome arm m, we locate two points j and l on the same arm such that j = i − 10 and l = i + 10 which, because the sampling interval is 0.1 μm, implies that points j, i, and l are separated from each other by a total contour length of 1 μm. We then compute the two successive tangent vectors u = r(i, m, t) − r(j, m, t) and v = r(l, m, t) − r(i, m, t). The angle θ between these tangents at point i can then be found as

$$\theta(i, m, t) = \cos^{-1}\{u \cdot v/||u||||v||\} \quad (9)$$

For each sampled point, traced over time, the average curvature is calculated over the entire time-series and used to compute the variance in curvature for that one point. The overall variance in curvature was then calculated by averaging the variances of all points on all chromosomes, based on the simplifying assumption that the bending modulus is similar for all chromosome segments.

One possible source of error is the interactive tracing of the chromosome backbone. Because this method relies on the user manually positioning the cursor in the apparent center of the chromosome cross section, random variation in exactly where a user positions the cursor during tracing could produce spurious variations in curvature. To estimate the contribution from such errors, a chromosome arm at a single time point was traced 11 separate times, and the same algorithm was used to measure the bending-angle variance. The variance in bending angle for a repeatedly traced arm was found to be just 0.002 ± 0.0002, a much smaller value than those measured in colchicine-treated or untreated embryos. This result implies that the process of interactive chromosome tracing is not a significant source of error.

We find the dynamic persistence length [36] from the variance in bending angle according to the relation

$$\rho = 2s/\langle\theta^2(s)\rangle \quad (10)$$

Dynamical model for thermal and random motor–driven bending fluctuations

We seek a model of bending fluctuations of an elastic filament, bent by both thermal and nonthermal microtubule/motor forces. Thermal forces are characterized by very short time (psec) and short distance (0.1 nm) correlations due to their origin in molecular motion. By contrast, microtubules and motors undergo processive driven reactions over distances of many nm. They can be expected to generate bursts of force with relatively long time correlations and with spatial correlations corresponding to the typical spacing between tubules or active motors.

The simplest equation of motion that takes all these factors into account is one that is essentially the standard thermal bending fluctuation model for stiff-rod polymers such as short dsDNAs, or actin filaments[37], plus non-thermal fluctuating driving forces. Chromosome motion is described by the displacement u(x, t) of the chromosome from its relaxed, straight configuration, which is a function of distance along the chromosome x, and time t:

$$\eta \frac{\partial u(x, t)}{\partial t} + A \frac{\partial^4 u(x, t)}{\partial x^4} + \sqrt{2\eta\, kT\, \nu}\,(x, t) + \frac{f}{\lambda}\sigma(x, t) = 0 \quad (11)$$

where η is the viscosity, A is the bending stiffness, k is Boltzmann's constant, T is the absolute temperature, and f and λ are the magnitude and spatial-correlation distance, respectively, of the nonthermal random force.

Note that although u in principle has two components, one in the plane of view and the other out of the plane, we consider only one component for simplicity, and the main results are not changed by this simplification. We also note that a similar model was introduced to describe cell membranes driven by nonthermal forces [38, 39].

Each term in Equation 11 is a contribution to the net force per length on the chromosome; inertia is neglected, as is usual in colloid and polymer physics [40] since the times at which free (inertial) motion occurs (∼psec) are far smaller than the time scales we observe experimentally (∼sec). The first term, proportional to the velocity of the chromosome point at (x, t), is the drag force per unit length, and therefore η is approximately the viscosity of the fluid surrounding the chromosome. The second term is the force that tends to make the chromosome straighten out due to its bending elasticity, described by the bending stiffness A [41]. These first two terms describe the overdamped motion of an elastic filament moving through a viscous medium.

The final two terms describe the random thermal and nonthermal motor/microtubule wind forces, respectively. The thermal force has zero mean, and its correlation function is $\langle\nu(x, t)\, \nu(x', t')\rangle = \delta(x - x')\, \delta(t - t')$, i.e., the thermal force is taken to have zero-range correlations in space and time. The amplitude of the thermal random force term is determined by the requirement that thermal equilibrium be reached, and it depends on the absolute temperature T.

The final fluctuating driving-force term is taken to have zero mean (in this treatment we consider only the period of metaphase, at which time there is no net drift of chromosomes through the cell) and finite-ranged correlations, with $\langle\sigma(x, t)\, \sigma(x', t')\rangle = \exp[-|x - x'|/\lambda] \exp[-|t - t'|/\tau]$. The length λ and time τ represent the distance and time over which microtubule growth or motors processively generate a force burst. In the case of microtubule growth, λ corresponds to the typical distance between adjacent microtubules pushing simultaneously on a chromosome, while τ would represent the duration of a single push imparted by one of those microtubules to the chromosome. The overall amplitude f is the average force contributed by a microtubule or motor during a single processive push.

This kind of equation is solved by the conversion of u(x, t) to its Fourier components u(q, ω):

$$u(q, \omega) = \int_{-\infty}^{\infty} dt \int_{0}^{L} dx\, u(x, t)\, e^{i(\omega t - qx)} \quad (12)$$

This allows the force equation to be reexpressed and solved in terms of u(q,ω) and the corresponding Fourier transforms of the random force functions:

$$u(q, \omega) = \frac{\sqrt{2\zeta\ kT}\, v(q, \omega) + (f/\lambda)\sigma(q, \omega)}{i\eta\omega - Aq^4} \quad (13)$$

Using the fact that the two types of thermal forces are uncorrelated allows the average correlation of u(q,ω) to be computed:

$$\langle u(q, \omega)\ u(q', \omega')\rangle = \frac{2\eta\ kT\,\langle v(q, \omega)\ v(q', \omega')\rangle + (f/\lambda)^2\,\langle \sigma(q, \omega)\ \sigma(q', \omega')\rangle}{A^2q^8 + \eta^2\omega^2} \quad (14)$$

After we plug in the random function correlation functions

$$<v(q, \omega)v(q', \omega')> = (2\pi)^2\ \delta(q + q')\ \delta(\omega + \omega') \quad (15)$$

and

$$<\sigma(q, \omega)\sigma(q', \omega')> = (2\pi)^2\ \delta(q + q')\ \delta(\omega + \omega') \times 4\lambda\tau/[(1 + \tau^2\omega^2)(1 + \lambda^2q^2)] \quad (16)$$

the time correlation function of the mode with wavenumber q, at two times t and t′ is:

$$\langle u(q, t)u(q, t')\rangle = \frac{(2\pi)^2\ \delta(q + q')}{Aq^4} \times \left[kTe^{-Aq^4|t - t'|/\eta} + \frac{2f^2\tau(e^{-Aq^4|t - t'|/\eta} - [Aq^4\tau/\eta]e^{-|t - t'|/\tau})}{\eta\lambda(1 + \lambda^2q^2)(1 - A^2q^8\tau^2/\eta^2)}\right] \quad (17)$$

The correlations are naturally strongest at t = t′, and they die away exponentially with the difference between the two times. The first term inside the square bracket is the usual thermal fluctuation result, It is proportional to the temperature T and shows that the typical lifetime for thermal fluctuations of modes of wavenumber q on an elastic filament is η/Aq^4.

The term that is proportional to f^2 is due to the nonthermal driving forces and itself is made up of two contributions. The first indicates the additional thermal-like fluctuations that are induced by the nonthermal forces. The second contribution decays with lifetime τ and indicates the direct contribution of the nonthermal forces to the bending fluctuations, and it is negligible for modes that satisfy $Aq^4\tau/\eta << 1$, i.e., modes with relaxation times longer than τ. This relation is satisfied for sufficiently small q values and thus for sufficiently long wavelengths.

Here we are concerned with fluctuations at one time, i.e., for t = t′, where the correlations are

$$\langle u(q, t)\ u(q', t)\rangle = (2\pi)^2\ \delta(q + q')\ \frac{kT}{Aq^4} \times \left[1 + \frac{2f^2\tau}{kT\eta\lambda}\,\frac{1}{(1 + \lambda^2q^2)(1 + Aq^4\tau/\eta)}\right] \quad (18)$$

To connect with the long-wavelength measurements of this paper, we consider the limiting behavior for small q values. In this limit, the effect of the nonthermal fluctuations is simply to reduce the persistence length from its thermal value A/kT by a factor $1 + 2f^2\tau/(kT\eta\lambda)$. We use only this persistence length "renormalization" result in the present paper, but it should be noted there are a number of other interesting features of this model. Such features include the strongly nonthermal fluctuation spectrum for large wavenumbers.

Acknowledgements

We thank Mats Gustafsson, Zvi Kam, Hao Li, and Orion Weiner for careful reading of the manuscript. This work was supported by grants from the National Institutes of Health (J. W. S.), the National Science Foundation (J. F. M.), the Whitaker Foundation (J. F. M.), the Petroleum Research Foundation of the American Chemical Society (J. F. M.) and by the Research Corporation (J. F. M.). D. A. A. was supported by the Howard Hughes Medical Institute. W. F. M. was a Howard Hughes Medical Institute predoctoral fellow and a Helen Hay Whitney Foundation postdoctoral fellow.

References

1. Hiraoka Y, Minden JS, Swedlow JR, Sedat JW, Agard DA: **Focal points for chromosome condensation and decondensation revealed by three-dimensional time-lapse microscopy.** *Nature* 1989, **342:**293-296.
2. Minden JS, Agard DA, Sedat JW, Alberts BM: **Direct cell lineage analysis in *Drosophila melanogaster* by time-lapse, three-dimensional optical microscopy of living embryos.** *J. Cell Biol.* 1989, **109:**505-516.
3. Swedlow JR, Sedat JW, Agard DA: **Multiple chromosomal populations of topoisomerase II detected in vivo by time-lapse, three-dimensional wide-field microscopy.** *Cell* 1993, **73:**97-108.
4. Thomas C, DeVries P, Hardin J, White J: **Four-dimensional imaging: computer visualization of 3D movements in living specimens.** *Science* 1996, **273:**603-607.
5. Alexander SP, Rieder CL: **Chromosome motion during attachment to the vertebrate spindle: initial saltatory-like behavior of chromosomes and quantitative analysis of force production by nascent kinetochore fibers.** *J. Cell Biol.* 1991, **113:**805-815.
6. Houchmandzadeh B, Marko JF, Chatenay D, Libchaber A: **Elasticity and structure of eukaryotic chromosomes studied by micromanipulation and micropipette aspiration.** *J. Cell Biol.* 1997, **139:**1-12.
7. Poirier M, Eroglu S, Chatenay D, Marko JF: **Reversible and irreversible unfolding of mitotic newt chromosomes by applied force.** *Mol. Biol. Cell* 2000, **11:**269-276.
8. Nicklas RB: **Chromosome velocity during mitosis as a function of chromosome size and position.** *J. Cell Biol.* 1965, **25:**119-135.
9. Nicklas RB: **Measurement of the force produced by the mitotic spindle in anaphase.** *J. Cell Biol.* 1983, **97:**542-548.
10. Skibbens RV, Skeen VP, Salmon ED: **Directional instability of kinetochore motility during chromosome congression and segregation in mitotic newt lung cells: a push-pull mechanism.** *J. Cell Biol.* 1993, **122:**859-876.
11. Gittes F, Mickey B, Nettleton J, Howard J: **Flexural rigidity of microtubules and actin filaments measured from thermal fluctuations in shape.** *J. Cell Biol.* 1993, **120:**923-934.
12. Houchmandzadeh B, Dimitrov S: **Elasticity measurements show the existence of thin rigid cores inside mitotic chromosomes.** *J. Cell Biol.* 1999, **145:**215-223.
13. Grosberg AYu, Khoklov AR: *Statistical physics of macromolecules.* New York: American Institute of Physics Press; 1994.
14. Luby-Phelps K: **Physical properties of cytoplasm.** *Curr. Opin. Cell Biol.* 1994, **6:**3-9.
15. Oegema K, Marshall WF, Sedat JW, Alberts BM: **Two proteins that cycle asynchronously between centrosomes and nuclear structures: *Drosophila* CP60 and CP190.** *J. Cell Sci.* 1997, **110:**1573-1583.
16. Berg H: *Random walks in biology*. Princeton, New Jersey: Princeton University Press; 1983.
17. Zhang P, Knowles BA, Goldstein LSB, Hawley RS: **A kinesin-like protein required for distributive chromosome segregation in *Drosophila*.** *Cell* 1990, **62:**1053-1062.
18. Vernos I, Raats J, Hirano T, Heasman J, Karsenti E, Wylie C: **Xklp1, a chromosomal *Xenopus* kinesin-like protein essential for spindle organization and chromosome positioning.** *Cell* 1995, **81:**117-127.
19. Murphy TD, Karpen GH: **Interactions between the nod+ kinesin-like gene and extracentromeric sequences are required for transmission of a *Drosophila* minichromosome.** *Cell* 1995, **81:**139-148.
20. Afshar K, Barton NR, Hawley RS, Goldstein LSB: **DNA binding and meiotic chromosomal localization of the *Drosophila* nod kinesin-like protein.** *Cell* 1995, **81:**129-138.
21. Ault JJG, Demarco AJ, Salmon ED, Rieder CL: **Studies on the ejection properties of asters: astral microtubule turnover influences the oscillatory behavior and positioning of mono-oriented chromosomes.** *J. Cell Sci.* 1991, **99:**701-710.
22. Rieder CL, Salmon ED: **Motile kinetochores and polar ejection forces dictate chromosome position on the vertebrate mitotic spindle.** *J. Cell Biol.* 1994, **124:**223-233.
23. Moritz M, Braunfeld MB, Fung JC, Sedat JW, Alberts BM, Agard DA: **Three-dimensional structural characterization of centrosomes from early *Drosophila* embryos.** *J. Cell Biol.* 1995, **130:**1149-1159.

24. Paddy MR, Saumweber H, Agard DA, Sedat JW: **Time-resolved, in vivo studies of mitotic spindle formation and nuclear lamina breakdown in *Drosophila* early embryos.** *J. Cell Sci.* 1996, **109:**591-607.
25. Hayden JH, Bowser SS, Rieder CL: **Kinetochores capture astral microtubules during chromosome attachment to the mitotic spindle: direct visualization in live newt lung cells.** *J. Cell Biol.* 1990, **111:**1039-1045.
26. Kuo SC, Sheetz MP: **Force of single kinesin molecules measured with optical tweezers.** *Science* 1993, **260:**232-234.
27. Svoboda K, Block SM: **Force and velocity measured for single kinesin molecules.** *Cell* 1994, **77:**773-784.
28. Hall K, Cole D, Yeh Y, Baskin RJ: **Kinesin force generation measured using a centrifugal microscope sperm-gliding motility assay.** *Biophys. J.* 1996, **71:**3467-3476.
29. Dogterom M, Yurke B: **Measurement of the force-velocity relation for growing microtubules.** *Science* 1997, **278:**856-860.
30. Fygenson DK, Marko JF, Libchaber A: **Mechanics of microtubule-based membrane extension**. *Phys Rev Lett* 1997, **79:**4497-4500.
31. Theurkauf WE, Heck MMS: **Identification and characterization of mitotic mutations in *Drosophila*.** *Meth Cell Biol* 1999, **61:**317-346.
32. Tvaruskó W, Bentele M, Misteli T, Rudolf R, Kaether C, Spector DL, *et al.*: **Time-resolved analysis and visualization of dynamic processes in living cells**. *Proc. Natl. Acad. Sci. USA* 1999, **96:**7950-7955.
33. Agard DA, Hiraoka Y, Shaw P, Sedat JW: **Fluorescence microscopy in three dimensions**. *Meth Cell Biol* 1989, **30:**353-377.
34. Chen H, Hughes DD, Chan TA, Sedat JW, Agard DA: **IVE (image visualization environment): A software platform for all three-dimensional microscopy applications.** *J Struc Biol* 1996, **116:**56-60.
35. Marshall WF, Agard DA, Sedat JW: **Quantitative analysis of chromosome motion in *Drosophila* melanogaster**. *Proc Soc Photo-optical Instr Eng* 1995, **2412:**33-34.
36. Bednar J, Furrer P, Katrich V, Stasiak AZ, Dubochet J, Stasiak A: **Determination of DNA persistence length by cryo-electron microscopy. Separation of the static and dynamic contributions to the apparent persistence length of DNA.** *J. Mol. Biol.* 1995, **254:**579-594.
37. Harnau L, Reineker P: **Equilibrium and dynamical properties of semiflexible chain molecules with confined transverse fluctuations.** *Phys Rev E* 1999, **60:**4671-4676.
38. Prost J, Bruinsma R: **Shape fluctuations of active membranes**. *Europhys Lett* 1996, **33:**321-326.
39. Prost J, Manneville JB, Bruinsma R: **Fluctuation-magnification of non-equilibrium membranes near a wall.** *Eur Phys J B* 1998, **1:**465-480.
40. Doi M, Edwards SF: *The Theory of Polymer Dynamics*. New York: Oxford University Press; 1986:Chs. 3-4.
41. Landau LD, Lifshitz EM: *Theory of elasticity,* 3rd edn. Elmsford, New York: Pergamon Press; 1986:64-67.